

**THE GENERATION OF ISOTROPIC TURBULENCE  
IN THE HIGH SPEED CASCADE WIND TUNNEL**

**P. Acton , L. Fottner  
Universität der Bundeswehr München  
Germany**

# The Generation of Isotropic Turbulence in the High Speed Cascade Wind Tunnel

Paola Acton and Leonhard Fottner  
Institut für Strahlantriebe  
Universität der Bundeswehr München  
85577 Neubiberg  
Germany

## ABSTRACT

Boundary layer transition in turbomachines strongly depends on the Reynolds number, on the Mach number as well as on the turbulence level. In order to make cascade measurements transferable to turbomachines it is necessary to achieve high turbulence levels in cascade wind tunnels. Therefore two passive turbulence generators were designed for the High Speed Cascade Wind Tunnel (HGK) of the University of the Federal Armed Forces Munich to create turbulence levels in the order of 8%. Particular emphasis was placed on the generation of a homogeneous turbulent flow field and on isotropic turbulence.

The three-dimensional hot wire anemometry was applied in order to evaluate the quality of the flow generated by the turbulence grids. This technique makes it possible to measure the 3D velocity vector as well as the three turbulence components in a small control volume. This way the flow structure inside the wind tunnel is investigated in detail.

Measurements were performed across the whole test section of the HGK in order to obtain information about the complete flow field of the wind tunnel.

The results of the new turbulence generators were also compared with those of two older ones which have been used for the last years. The mean turbulence level achieved by the new turbulence generators is respectively 7% and 9%. Both a uniform as well as a nearly isotropic flow field is obtained and therefore a new turbulence generator will be used during the next tests on cascades.

## NOMENCLATURE

### Symbols:

$b$  [mm] width or diameter of bars

$dTu_{u-v}$ [%]	deviation from isotropy
$dTu_{u-w}$ [%]	deviation from isotropy
$dTu_{v-w}$ [%]	deviation from isotropy
$g$ [m/s]	velocity
$n$ [-]	contraction ratio
$p$ [hPa]	static pressure
$u$ [mm]	coordinate in circumferential direction
$u, v, w$ [m/s]	$x$ -, $y$ -, $z$ -components respectively of the fluctuating velocities
$x$ [mm]	coordinate in axial direction, distance from turbulence generator in axial direction
$C$ [-]	constant for the calculation of the turbulence level
$H$ [mm]	height of wind tunnel
$M$ [mm]	mesh length of grid
$Re/l$ [1/m]	Reynolds number per unit length
$T$ [°C]	static temperature
$Tu$ [%]	turbulence level
$U, V, W$ [m/s]	velocity components respectively in $x$ -, $y$ -, $z$ -direction
$\beta$ [-]	grid porosity
$\nu$ [m <sup>2</sup> /s]	kinematic viscosity
$\Delta Tu$ [%]	deviation from the mean value of the turbulence level

### Subscripts:

0	reference conditions
1	upstream conditions
$u$	component in $x$ direction
$v$	component in $y$ direction
$w$	component in $z$ direction

### Abbreviations:

3D	three dimensional
HFA	Hot Film Anemometry
HGK	High Speed Cascade Wind Tunnel
RMS	Root Mean Square
Ma	Mach number

## INTRODUCTION

For the optimization of turbomachinery blades it is useful to get a good insight in the phenomenon of transition. Detailed analyses have already been performed on the influence of Mach and Reynolds number as well as of incidence angle on the boundary layer behavior of turbine blades. Despite of the high turbulence levels characterising the flow especially in high pressure turbines their effect on transition was scarcely investigated before. In this paper the design of turbulence generators for the HGK (High Speed Cascade Wind Tunnel) is presented together with the results of their first test cases. A turbulence intensity of 8% was achieved in the test section of the wind tunnel. When designing the turbulence generator -or grid- particular effort was put on the uniformity of the velocity and turbulence flow field.

The most common turbulence generators have the form of grids. They are applied in wind tunnels for different purposes: either to modify the velocity profile or to enhance or to dump turbulent energy. In any case they cause a pressure loss in the tunnel. Though they have been analysed for years it is still almost impossible to describe grids' behaviour analytically and just few doubtful empirical correlations are known to predict the flow characteristics behind grids. In previous research work most authors just analysed the pressure loss across the grid (Pinker and Herbert, 1966; 1967; Cornell, 1958) or the turbulence generation (Kistler and Vrebalovich, 1966; Gad-El-Hak and Corrsin, 1974; Blair et al., 1981; Blair and Werle, 1980) separately. Only few were concerned with both influences of a grid (Baines and Peterson, 1951; Kiock et al., 1982; Kotlarski, 1980). Scarce attention was drawn to the investigation of the whole flow field behind grids. Most measurements were performed only in the centre of the wind tunnel and the distribution was assumed to be uniform over the whole flow field. Only in Kiock et al. (1982), Kotlarski (1980), Freudenberg (1988), Dörr (1994) flow field measurements were performed covering the whole wind tunnel section and information about uniformity was given.

Some authors gave empirical correlations between the grid's geometry and the flow characteristics behind it but many problems may arise in the use of published correlations for the design of a turbulence generator.

- In most cases just one generators' geometry was analysed: Crossed or parallel grids of round or square bars, so that the resulting correlations would be applicable just in some limited cases.
- For a number of references, use has been made of a wind tunnel having relatively large background turbulence energy. In those cases the generated turbulence energy can be significantly increased above that which would be otherwise obtained.

- The dimension of the grid in respect to the channel's dimensions plays an outstanding role: If the mesh size is not smaller than 10% of the tunnel's hydraulic diameter turbulence can be strongly inhibited.

In most quoted references the importance of observing tight tolerances in the mesh width and bar diameter (or bar width) of the grid has been pointed out. Even slight deviations of the geometry can have significant influence on the downstream turbulence characteristics.

## HIGH SPEED CASCADE WIND TUNNEL (HGK)

The High Speed Cascade Wind Tunnel of the University of the Federal Armed Forces Munich is one of few facilities which enable the independent variation of Mach and Reynolds number (see Sturm and Fottner, 1985). This is possible because the tunnel is installed in a pressure tank, which can be evacuated down to 40 hPa and pressurised up to 1200 hPa.

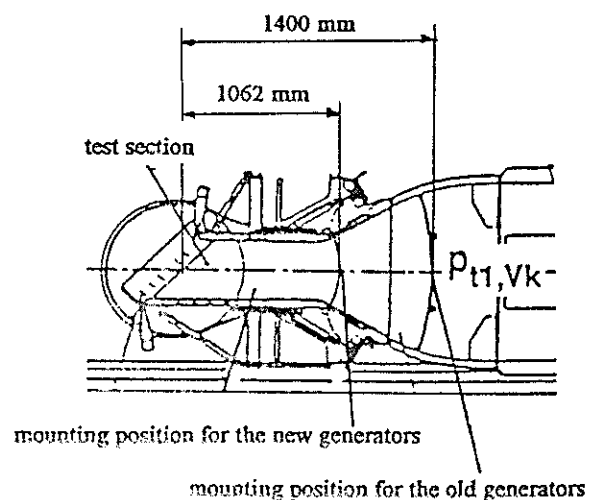


Fig 1 The test section of the HGK and the position of the turbulence generators

The air -supplied by a six-stage axial compressor- flows through a diffuser into a settling chamber, where it is cooled to a constant air temperature of 40°C, and through a nozzle of variable height so that the test section's dimensions can vary between 250 mm x 300 mm and 500 mm x 300 mm. The wind tunnel can operate continuously and is an open loop system in a closed test facility.

Until now turbulence has been generated by grids inserted in the nozzle at a distance of 1400 mm from the

test section (Fig.1). The maximum level already reached was of 6.8%.

### GENERATION OF HIGH TURBULENCE LEVELS IN THE HGK

Intending to simulate the flow conditions in a high pressure turbine by wind tunnel testing high turbulence levels are necessary in the test section. With regard to the big difficulties in generating high turbulence intensities, a turbulence level of ca. 8% was fixed as desirable in the HGK's test section. Great care was put on generating a most uniform and isotropic flow field. Already at this point it has to be emphasised that the generation of high turbulence levels combined with great demands on the uniformity of the flow field is very difficult to accomplish.

The different testing conditions of the HGK ( $p_1$  i.e.  $Re_1$ ,  $Ma_1$ ) as well as the test section's variable geometry may give rise to different turbulence structures even for the same generator. The test section's height influences the contraction of the nozzle and therefore can inhibit more or less strongly the turbulence generation. The effect of Mach and Reynolds numbers still has not been analysed definitely.

With respect to these considerations turbulence generators which can change their characteristics continuously with the test conditions seem to be useful. One example for such generators are "active" ones. They generate turbulence by blowing small jets into the primary flow. The interaction between the two flows, characterised by different velocities, generates vortices which can enhance turbulence up to 40%. Such generators have already been developed and tested by Gad-El-Hak and Corrsin, 1974; Freudenberg, 1988; Dörr, 1994; Tasso and Kamotani, 1975. All authors pointed out the difficulty in obtaining a uniform flow field. Gad-El-Hak and Corrsin, 1974 solved the problem only by regulating each jet separately with one valve.

Because of the difficulty in the application of active turbulence generators and because of the complexity of their implementation in the HGK "passive generators" i.e. grids have been chosen for our purpose. Even though it is not possible to regulate these generators, they have the advantage of being constructed more easily and with tighter tolerances, which will improve the quality and the uniformity in the flow field.

The turbulence generators have been designed for the following tunnel's working conditions:  $H=493$  mm,  $Ma_1=0.28$ ,  $p_1=150$  hPa (i.e.  $Re_1/l=5 \cdot 10^5$ ), corresponding to the design point of the turbine cascade T106-300. For these flow conditions the turbulence grids already

available VIk and IXgk (Fig.2a) generate respectively  $Tu_{uVIk}=4.2\%$ ,  $Tu_{uIXgk}=6.8\%$  while the new one should generate 8% turbulence or more.

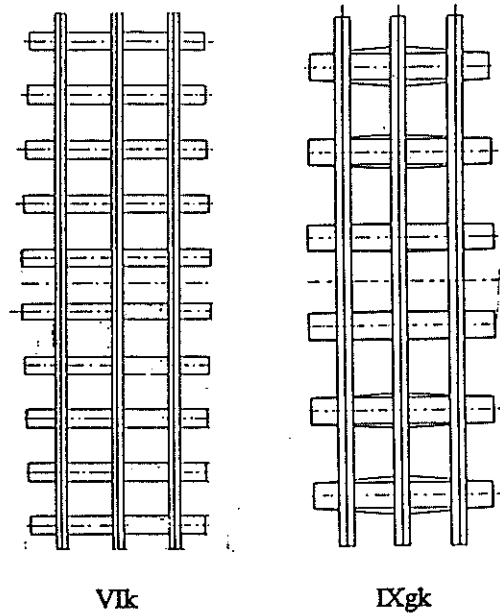


Fig.2a The turbulence generators VIk, IXgk

The new generators were designed in conformity with the correlation from Roach, 1987. This reference is the most recent and detailed synthesis of experimental data regarding the flow through grids. The proposed correlations are very simply applicable and already tested in their reliability from Gregory-Smith and Cleak, 1990.

The general correlation for the calculation of the turbulence level following Roach, 1987 is:

$$Tu_u = C \left( \frac{x}{b} \right)^{-5/7}$$

where  $Tu_u$  is the turbulence's component in u-direction defined as follows:

$$Tu_u = \sqrt{\frac{u'^2}{U}}$$

$x$  is the distance between generator and test section and  $b$  is a characteristic grid dimension as diameter or bar width. The "constant"  $C$  is a function of grid geometry and reflects the drag force experienced by individual (isolated) elements of the grid.

Designing a turbulence generator some boundary conditions have to be respected and some general rules

have to be followed, which often stand in contrast to each other:

- The smallest distance between generator and test section is fixed by the tunnel's geometry (adjustable lower and upper walls) and amounts to 1062 mm. In order to make it possible for the vortices to mix and to generate a uniform flow it is recommended to put the generator at least 10 mesh sizes upstream from the test section.
- The grid's porosity  $\beta$  (ratio between open section and grid's total section) has to be bigger than 0.6 in order to generate a uniform velocity and turbulence profile.
- The bar's width depends only on the desired turbulence level, once the geometry and the location of the generator have been decided.

The new generators are installed downstream of the nozzle, 1062 mm upstream of the test section with a grid dimension of 300 mm x 550 mm. This position was chosen to minimise the nozzle's dumping effect and to be as near as possible to the test section. To avoid the risk of a non-uniform flow a high grid porosity was chosen and high standards were put for the grid's manufacture.

With regard to the boundary conditions given by the HGK, grids made of parallel and squared bars have been preferred to those made of round and crossed bars, as they can produce higher turbulence levels for a chosen grid porosity. Furthermore using square bars the dependence between the generated turbulence intensity and the Reynolds number is very low, as the separation point is fixed geometrically and does not depend on the flow velocity and density. The question if the choice of parallel instead of crossed grids could cause a more anisotropic flow is denied by Roach, 1987 and will be analysed in the following.

For the chosen geometry (square and parallel bars) the correlation becomes:

$$Tu_u = 1.2 \left( \frac{x}{b} \right)^{-5/7}$$

Taking into account the boundary conditions and the quoted equations, having fixed the geometry of the grid and with a desired turbulence intensity of 8% only the bar's width remains unknown. As the generator is mounted inside the tunnel's nozzle the contraction effects have to be considered, for example by the following equation from Rannacher, 1982:

$$\frac{Tu}{Tu_0} = \frac{\sqrt{\frac{1}{3} \left( 2n + \frac{1}{n^2} \right)}}{n}$$

where  $n$  is the contraction ratio,  $Tu_0$  is the turbulence intensity for a constant section and  $Tu$  is the turbulence intensity behind the nozzle. Here we have a contraction of  $n=1.1$  and therefore  $Tu/Tu_0=0.90$ , which will be applied in the following calculations.

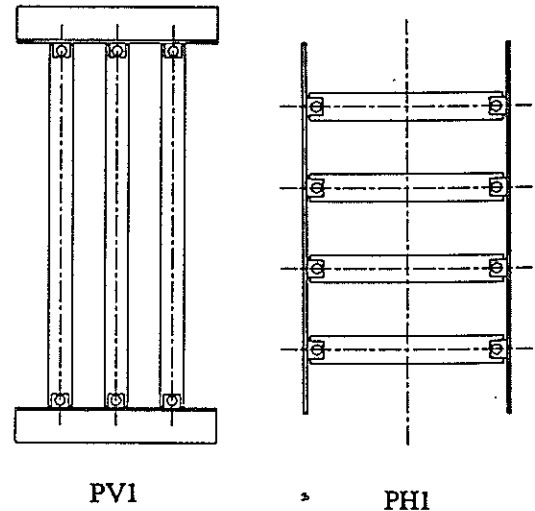


Fig.2b The turbulence generators PV1 and PH1

Two generators have been designed: PV1 and PH1. The first, PV1, consists of 35 mm thick bars which are positioned vertically in the tunnel. Thus possible wakes affecting the cascade can be minimized. The bars are curved in a circular shape so that the flow in the nozzle is always perpendicular to the grid. The second, PH1, consists of 40 mm thick bars which are positioned horizontally in the tunnel. A higher risk of strong wakes is present but a much more precise construction is possible in order to produce a uniform flow field.

The geometry as well as the calculated fluid dynamic characteristics of the two new turbulence generators are listed in Tab.1 and sketched in Fig.2b.

	PV1	PH1
b [mm]	35.00	40.00
M [mm]	88.75	118.00
x/M	11.9	9.0
Tu <sub>u</sub> [%]	6.6	7.2
Tu <sub>v</sub> [%]	7.4	8.1
Tu <sub>w</sub> [%]	7.4	8.1
$\Delta p/q$	1.59	1.27
$\beta$	0.61	0.66

Tab.1 Geometrical and fluid dynamic characteristics of the generators PH1 and PV1

## EXPERIMENTAL SET UP

The turbulence measurements were performed with the help of the 3D Hot Film Anemometry system (3D-HFA) which was developed by Rosemann, 1989 and Wunderwald et al., 1992 during previous research work. The hot film probe 55R91 from DANTEC was employed during these tests. The data acquisition as well as the automatic probe traversing was performed by the program SMASH which was developed at the Institute by Wunderwald et al., 1992.

The measurements were carried out in the open test section of the wind tunnel (H=493 mm) for the following flow conditions:  $Ma_1=0.28$ ,  $p_1=150$  hPa,  $T_1=40^\circ\text{C}$ . The hot film probe was held in the test section from downstream and positioned automatically. One turbulence generator at a time was installed in the tunnel and its flow field was traversed with the 3D probe 391 mm in u-direction and 216 mm in z-direction (corresponding to the maximum traversing distance of the traversing mechanism). The distance between two adjacent measurement points was chosen as a compromise between a detailed flow field map and the necessity of observing the measurement time:  $\Delta u=23$  mm and  $\Delta z=18$  mm, which led to the total number of measurement points of 234 (Fig.3).

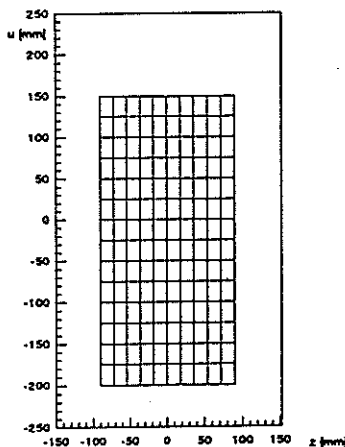


Fig.3 The measurement matrix of the test section

A sampling frequency of 32768 Hz was selected together with a measurement time of 1.5 s, which led to a measurement and acquisition time of 3 hours for each channel setting.

## RESULTS AND DISCUSSIONS

In the following the results of all four turbulence generators (VIk, IXgk, PVI and PH1) are summarised in one figure for each analysed quantity. The diagram

position in the figure has always to be correlated to the same turbulence grid as sketched in Fig.2a,b.

### Velocity Distribution

From 3D HFA measurements it is possible to determine the three velocity components. The velocity's magnitude  $g$  is defined to:

$$g = \sqrt{U^2 + V^2 + W^2}$$

In Fig.4a the percentage deviation from the average velocity:

$$\Delta g = \frac{g(u,z) - \bar{g}}{\bar{g}} 100\%$$

is plotted for the generator PH1.

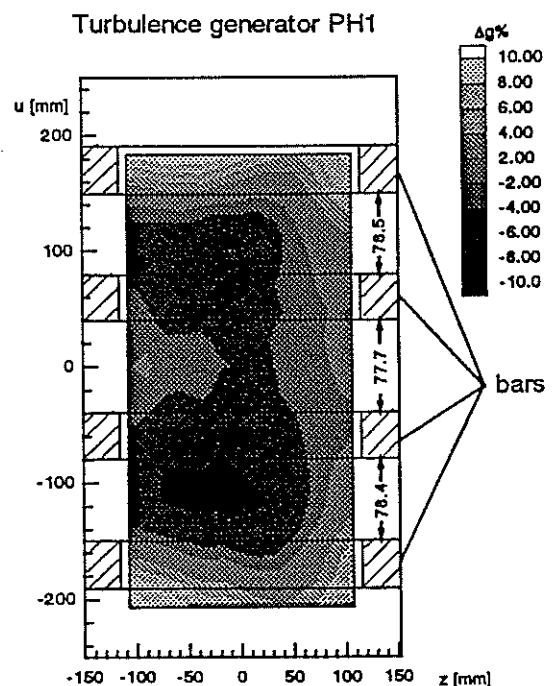


Fig.4a Distribution of percentage deviation from average velocity behind the PH1 with superimposed generator's geometry before the bars' adjustment

The results are given in form of contour-plots of different grey-levels and to characterise deviations bigger than 10% black or white colour is chosen. The blade's height direction  $z$  is plotted on the abscissa and the circumferential direction  $u$  on the ordinate. The outer black frame gives the dimensions of the test section the inner one those of the traversed field.

The generator's geometry is superimposed to the contour plot and shows a clear correlation between the bars' spacing and velocity: In locations where the bars are nearer to each other the velocity is higher. Therefore a locating jig was employed to secure the grid bars at precise intervals and the measurements were repeated. As shown in Fig.4b a much better velocity distribution was reached by the precise positioning of the bars. In this way the importance of a very accurate manufacturing of the grids could be underlined again.

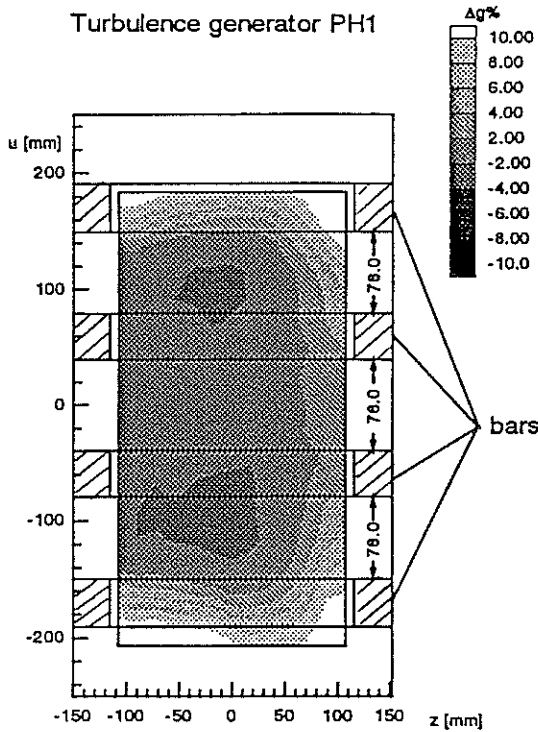


Fig.4b Distribution of percentage deviation from average velocity behind the PH1 with superimposed generator's geometry after the bars' adjustment

Fig.5 shows the distribution of the percentage deviation of the velocity for all turbulence generators. Vlk clearly shows the most uniform velocity distribution, the new PV1 the worst. The biggest deviations of the IXgk and the PH1 are of the same magnitude. The velocity distribution of the PH1 shows a slight periodicity in z-direction, which might depend on the generator's geometry (only horizontal bars).

**Turbulence Distribution**

3D HFA measurements enable the determination of all three components of the turbulence. Therefore not only the turbulence intensity:

$$Tu = \frac{\sqrt{u^2 + v^2 + w^2}}{3g}$$

was calculated but also its three components  $Tu_u$ ,  $Tu_v$  and  $Tu_w$  respectively in x-, u- and z-direction (see Fig.6):

$$Tu_u = \frac{\sqrt{u^2}}{U} \quad Tu_v = \frac{\sqrt{v^2}}{V} \quad Tu_w = \frac{\sqrt{w^2}}{W}$$

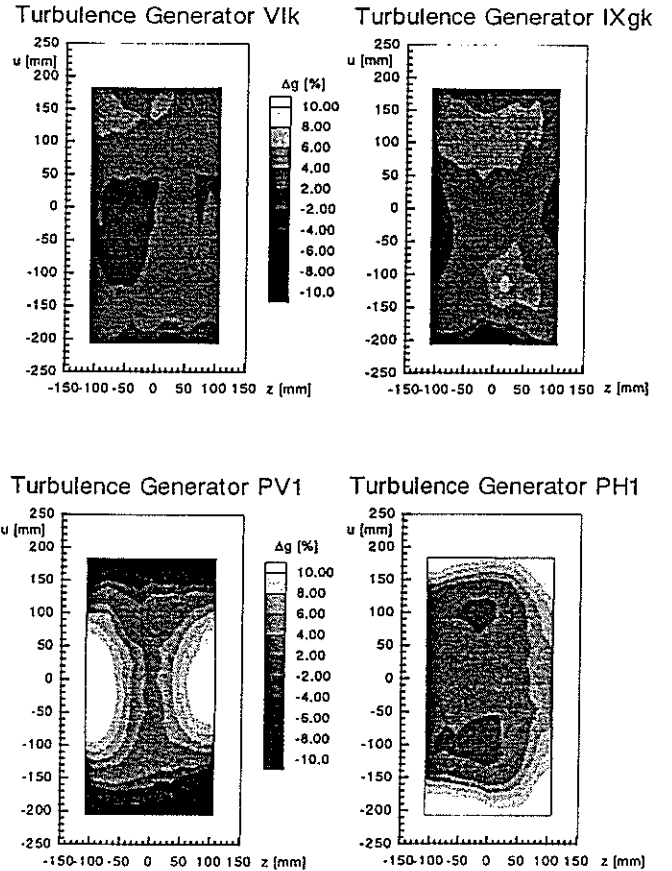


Fig.5 Distribution of the percentage deviation of the velocity Δg%

It is necessary to start with the representation of the absolute turbulence intensity. In Tab.2 the average of the turbulence level and its three components is summarised for all four generators. It is evident that both new turbulence grids generate the desired turbulence levels. The difference between measured and calculated values may depend on the use of empirical formulas and on the particular geometry of the wind tunnel.

	Tu	$Tu_u$	$Tu_v$	$Tu_w$
Vlk	4.2	3.8	4.8	3.9
IXgk	6.8	6.5	7.6	6.1
PV1	7.5	7.8	7.4	7.3
PH1	8.8	9.1	9.1	8.1

Tab.2 Mean Values of the turbulence levels of the four generators

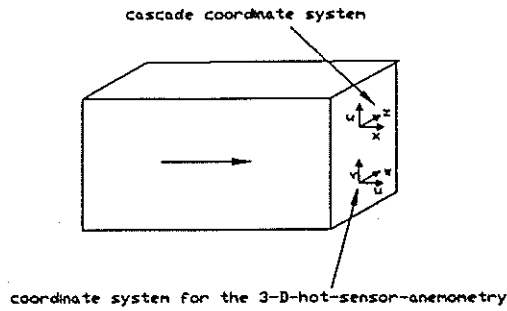


Fig.6 Reference system in the test section

In Fig.7 the absolute values of the turbulence level are represented in form of contour plots in which the total deviation region of the turbulence intensity is represented from black to white. As the difference between two contour lines represents the same percentage part of the average turbulence of each generator, a different number of grey levels is represented in every plot.

Relative quantities are necessary to compare the quality of the four turbulence generators. Therefore the percentage difference from the mean value was calculated:

$$\Delta Tu = \frac{Tu(u,z) - \bar{Tu}}{\bar{Tu}} 100\%$$

For the representation of these quantities the contour levels have been chosen so that the values between -5% and +5% are plotted in one colour (as these values are inside the measurement accuracy) and the grey levels are then in 5% steps. The values above 10% or smaller than -10% are characterised by white or black colour in order to mark them as "bad values" (Fig.8). Tab.3 summarises the maximum deviations from the average value.

	Tu	Tu <sub>u</sub>	Tu <sub>v</sub>	Tu <sub>w</sub>
Vlk	-16.8	-13.9	-26.1	-15.9
	22.4	61.4	22.2	33.9
IXgk	-17.2	-16.0	-25.8	-14.0
	28.5	49.7	14.6	39.5
PVI	-18.9	-22.3	-12.3	-25.6
	34.9	50.5	25.4	29.4
PH1	-16.3	-13.5	-18.7	-20.1
	10.4	11.5	11.1	12.0

Tab.3 Maximum percentage deviation from the mean value of the turbulence level of the four turbulence generators

The generator PH1 shows the most uniform distribution of the turbulence intensity with just some traces of irregularities in u-direction. The Vlk generates a distribution with nonuniformities in z-direction, while IXgk and PVI generate strange, almost point-symmetrical distributions with strong deviations from mean value, which cannot be directly explained by the grid's geometry.

The quality of the turbulence distribution can be summarised with help of the RMS:

$$\bar{s} = \sqrt{\frac{1}{n} \sum_{i=1}^n (Tu_i - \bar{Tu})^2}$$

where n is the number of points of the measurement matrix.

The calculated values are listed in Tab.4. The generator PH1 shows the lowest RMS value for all turbulence components and therefore the most uniform distribution. The generators PVI and Vlk exhibits strong nonuniformities and the IXgk generates a satisfactory distribution.

	Tu	Tu <sub>u</sub>	Tu <sub>v</sub>	Tu <sub>w</sub>
Vlk	8.1	11.3	10.8	7.9
IXgk	7.0	9.7	8.7	11.5
PVI	10.9	15.1	8.5	10.7
PH1	4.6	5.2	5.6	5.4

Tab.4 RMS values of the turbulence values of all generators

In Figs.9, 10, 11 the distribution of the three turbulence components is plotted regarding the same rules as in Fig.8. In this case the PH1 also produces the best distribution, the Vlk a satisfactory one and the IXgk and PVI the worst. It is interesting that using the PH1 the distributions of all three components have almost the same structure. In contrast the other generators show very different patterns so that the anisotropy of the flow field can already be stated here.

#### Isotropy

A flow is called isotropic if its three components of turbulence are equal. In order to verify this characteristic in the HGK the local difference between two turbulence components was calculated and referred to the local mean value of both:

$$dT_{u-v} = \frac{Tu_u(u,z) - Tu_v(u,z)}{\frac{1}{2}(Tu_u(u,z) + Tu_v(u,z))} 100\%$$



$$dT_{u-w} = \frac{T_{u_z} - T_{w_z}}{\frac{1}{2}(T_{u_z} + T_{w_z})} 100\%$$

$$dT_{v-w} = \frac{T_{v_z} - T_{w_z}}{\frac{1}{2}(T_{v_z} + T_{w_z})} 100\%$$

	$dT_{u-v}$	$dT_{u-w}$	$dT_{v-w}$
Vlk	-24.3	-3.5	-15.9
IXgk	-16.1	5.6	21.7
PV1	4.3	5.3	1.0
PH1	-0.9	10.7	11.6

Tab.5 Maximum percentage deviation from isotropy of all generators

The results of this calculation have been evaluated in form of contour plots (Figs.12, 13, 14) as well as averaged in order to get a global information about the isotropy (Tab.5).

A superficial observation of the results is sufficient to note that the flow field is not isotropic and that this quantity is strongly dependent on the turbulence generator. Therefore no general statements can be made.

As expected the generators Vlk and IXgk behave in a similar manner because they have similar geometries and the same installation position in the tunnel. Following Roach, 1987 the v- and w-components should be equal and 1.2 times bigger than the u-component. The measurements confirm this assumption for the v-direction but not for the w-direction. The w-component is in the same order of magnitude as the u-component and therefore significantly smaller than the v-component. This might be provoked by the geometry of the generators which are mainly built of horizontal bars which give rise to vortices with high fluctuations in v-direction. It is worth while mentioning that the nozzle effect is not sufficient to damp these stronger fluctuations. With regard to the contour plots it can be seen that the isotropic characteristics are distributed almost uniformly over the whole test section even if the single turbulence components are not.

The explanation of the results of the generators PH1 and PV1 seems to be more difficult. Because of their position in the wind tunnel the nozzle effect is very small (contraction factor of 1.1) and the v-component of turbulence is less damped. The mean value of the deviation from isotropy is misleading in this case. Especially making use of the PV1 the isotropic characteristics of the flow field are distributed very irregularly over the test section and fluctuate very strongly between positive and negative values. The small mean value of the deviation

from isotropy is therefore not a sign of good isotropy but just the arithmetic average between strong positive and negative values. Furthermore it can be observed that not only the different components of turbulence are distributed in a very nonuniform way over the test section but also that the isotropy scatters in a wide range.

In comparison the deviation from isotropy of the generator PH1 has quite a uniform distribution, so the calculated mean values have also a physical meaning. The v- and w-components are in the same order of magnitude and slightly smaller than the u-component. The flow downstream of the PH1 is not only uniform distributed but also almost isotropic.

It should be mentioned that the considerations about the isotropy should not be an evaluation of the quality of the generators but just an information about the real flow field in the HGK. Furthermore it is important that isotropic characteristics will vary with the height of the wind tunnel's test section. In smaller test sections the nozzle influence in v-direction will be stronger dumping the v-component and generating a more isotropic flow field for the Vlk and the IXgk.

#### Reproducibility of the Measurements

In order to verify the measurements and to evaluate the quality of the measurement technique some re-measurements were performed after some weeks (series B). The hot film probe was calibrated again with respect to the directional characteristics as well as for the velocity magnitude. The wires were set to different positions in each of the two series. Grid PV1 was not measured in series B as it was already clear that it generates no satisfactory flow field. A smaller and less detailed measurement field was traversed behind the other turbulence generators for time reasons.

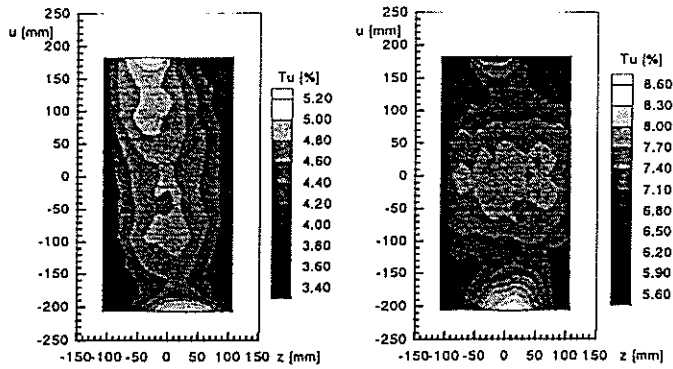
The comparison of the mean values of the two series is good, the differences vary generally in the range of a few percentage points maximum and are also a proof of the quality of the measurement technique (Tab.6).

		Tu	T <sub>u<sub>1</sub></sub>	T <sub>u<sub>v</sub></sub>	T <sub>u<sub>w</sub></sub>
Vlk	A	4.3	3.8	4.9	3.9
	B	4.3	4.7	5.1	4.1
IXgk	A	6.8	6.4	7.9	6.1
	B	7.0	6.3	8.0	6.7
PH1	A	8.8	9.0	9.2	8.2
	B	9.2	9.0	9.4	9.3

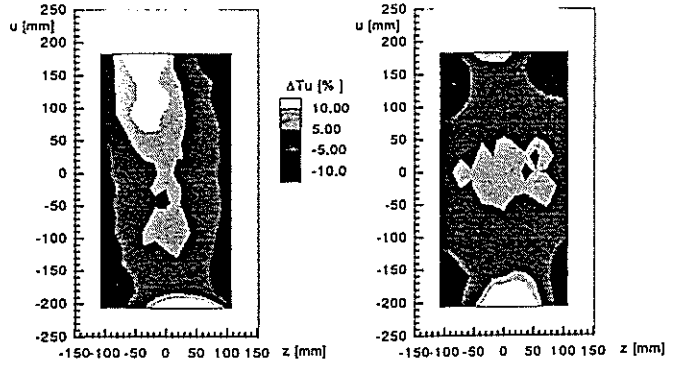
Tab.6 Comparison of the mean values of the two measurement series

Turbulence Generator VIK  
Average Tu-Level Tu = 4.2%  
Tu<sub>min</sub> = 3.5% Tu<sub>max</sub> = 5.3%

Turbulence Generator IXgk  
Average Tu-Level Tu = 6.8%  
Tu<sub>min</sub> = 5.5% Tu<sub>max</sub> = 8.7%

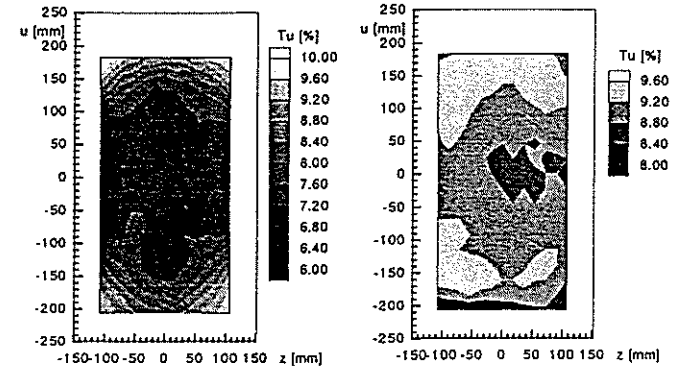


Turbulence Generator VIK      Turbulence Generator IXgk



Turbulence Generator PV1  
Average Tu-Level Tu = 7.5%  
Tu<sub>min</sub> = 6.1% Tu<sub>max</sub> = 10.1%

Turbulence Generator PH1  
Average Tu-Level Tu = 8.8%  
Tu<sub>min</sub> = 8.0% Tu<sub>max</sub> = 9.6%



Turbulence Generator PV1      Turbulence Generator PH1

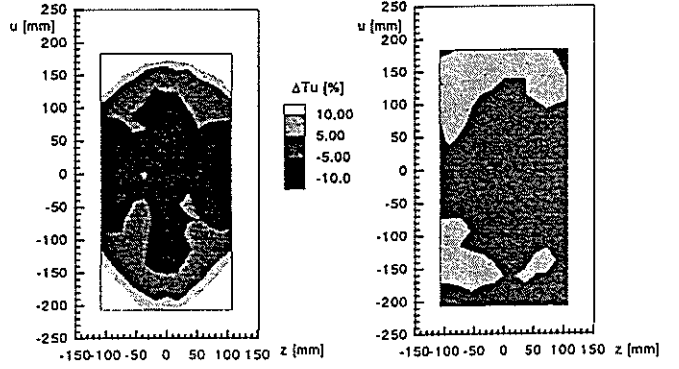
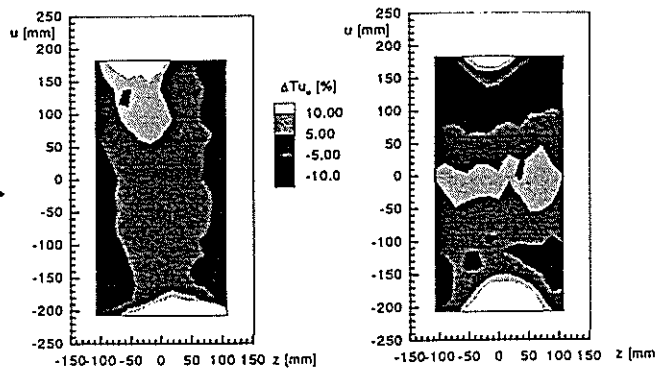


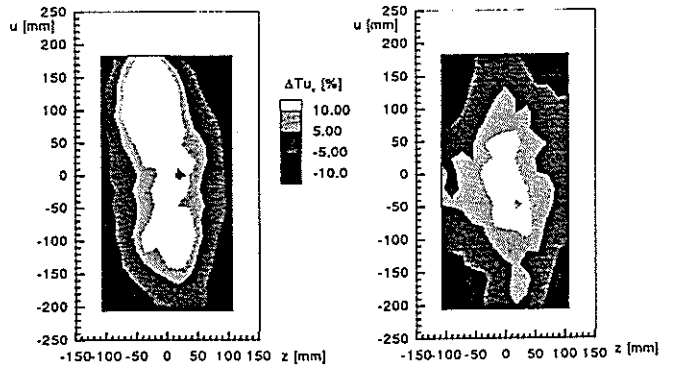
Fig.7 Distribution of the turbulence intensity Tu

Fig.8 Distribution of the percentage deviation of the turbulence intensity ΔTu%

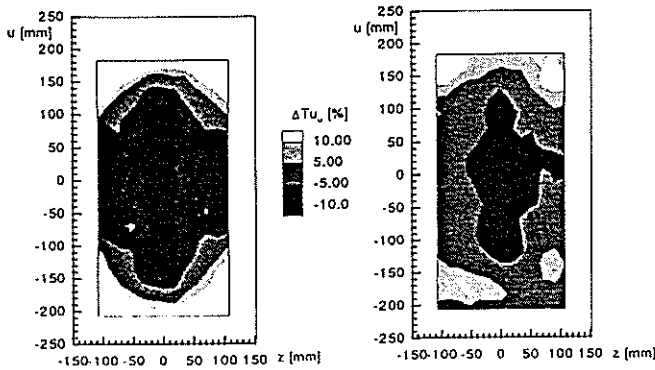
Turbulence Generator VIK      Turbulence Generator IXgk



Turbulence Generator VIK      Turbulence Generator IXgk



Turbulence Generator PV1      Turbulence Generator PH1



Turbulence Generator PV1      Turbulence Generator PH1

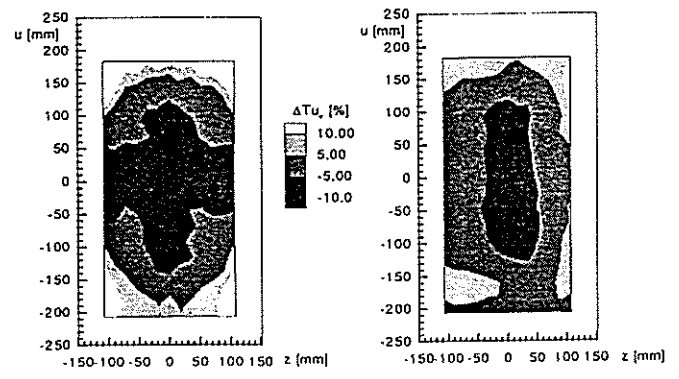


Fig.9 Distribution of the percentage deviation of the turbulence intensity ΔTu<sub>v</sub>%

Fig.10 Distribution of the percentage deviation of the turbulence intensity ΔTu<sub>v</sub>%

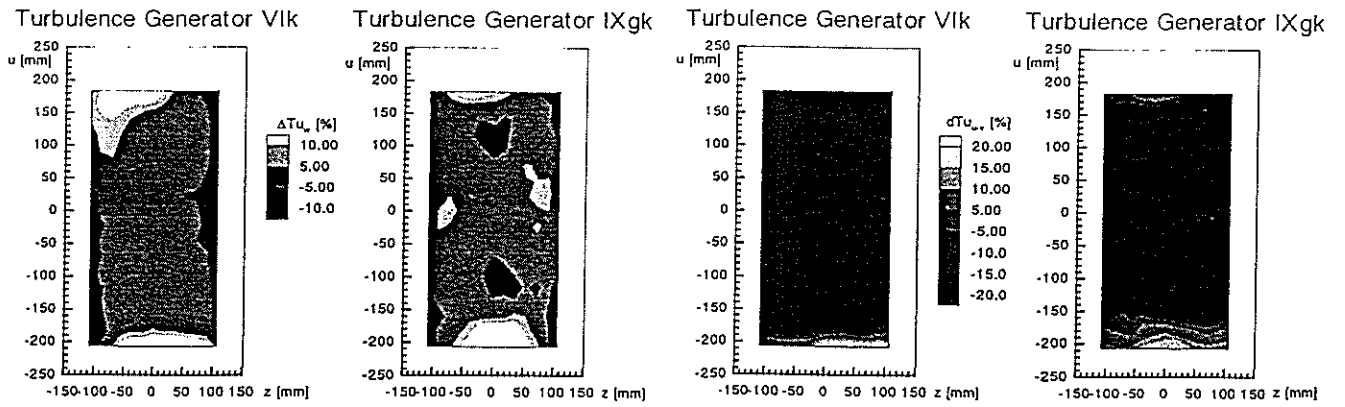


Fig.11 Distribution of the percentage deviation of the turbulence intensity  $\Delta Tu_w$  %

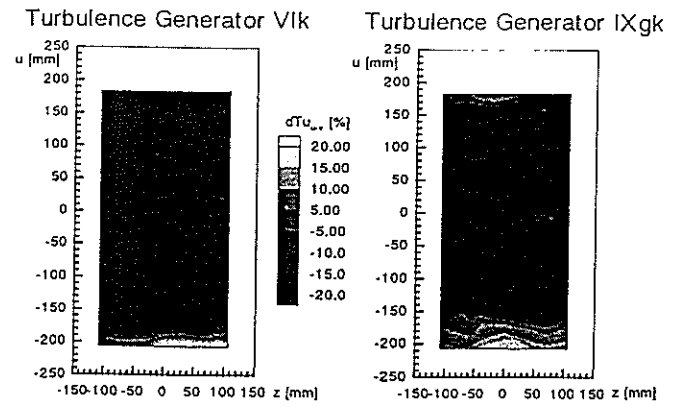


Fig.12 Distribution of the percentage deviation from isotropy  $dTu_{u-v}$  %

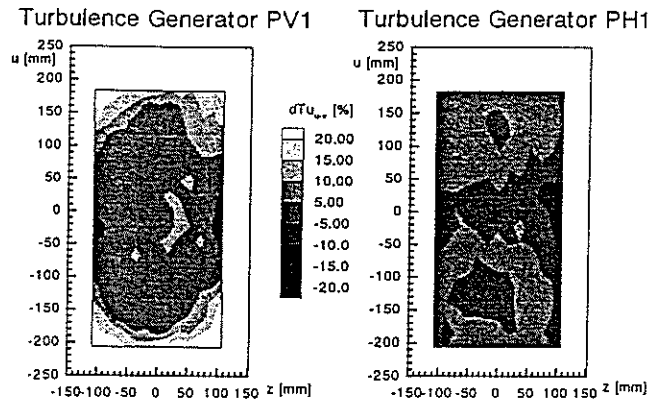
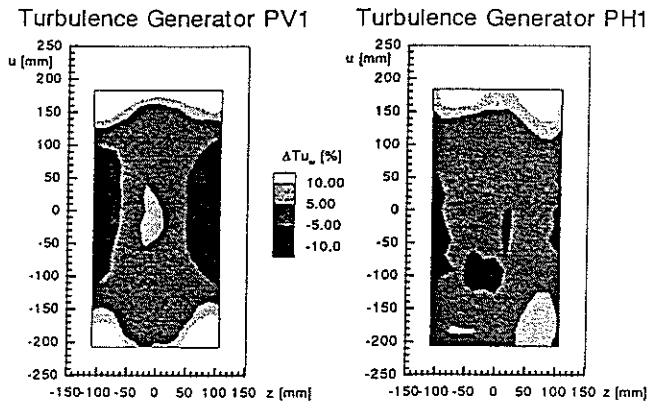


Fig.13 Distribution of the percentage deviation of the turbulence intensity  $\Delta Tu_w$  %

Fig.14 Distribution of the percentage deviation from isotropy  $dTu_{u-v}$  %

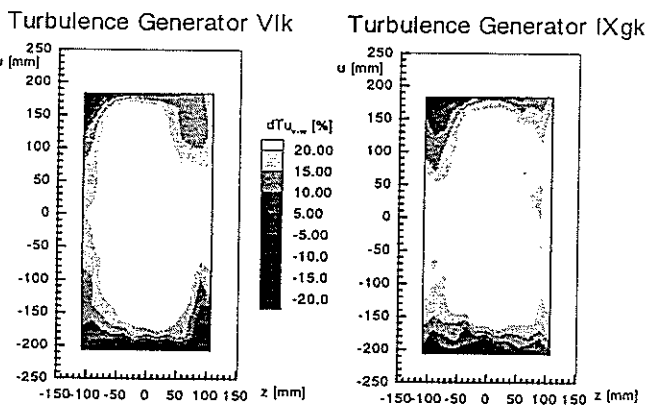
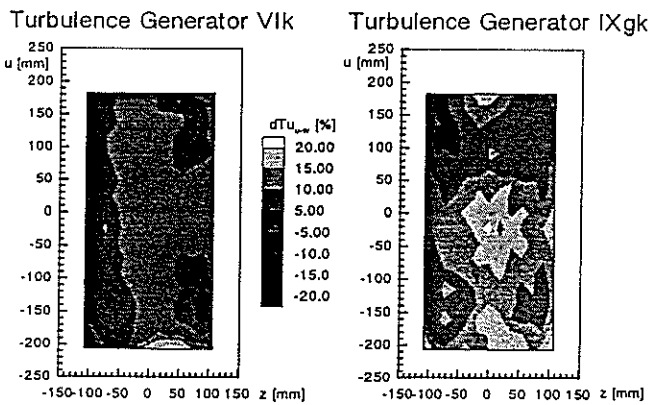


Fig.13 Distribution of the percentage deviation from isotropy  $dTu_{u-w}$  %

Fig.14 Distribution of the percentage deviation from isotropy  $dTu_{v-w}$  %

## SUMMARY

High turbulence intensities had to be achieved in the HGK with the new turbulence grids PV1 and PH1. To analyse the generated flow field velocity and turbulence measurements were performed behind the new generators as well as behind the old turbulence grids Vlk and IXgk. For that purpose the 3D-HFA has shown to be very suitable.

The flow fields generated by the four grids were analysed with respect to velocity, turbulence and isotropy. The grid PH1 could generate the desired turbulence level of 8%. Furthermore it showed the best turbulence distribution, a satisfactory velocity distribution, as well as an almost isotropic flow field.

The generator PV1 exhibited inadmissible nonuniformities in velocity and turbulence distribution so that it has to be excluded from the next use. The other generators showed good velocity distributions, satisfactory turbulence qualities and poor isotropic characteristics.

A better insight in the structure of the turbulence could be achieved by spectral analysis of the anemometry signals and will be performed soon.

## REFERENCES

- Baines, W.D., Peterson, E.G. (1951), "An Investigation of Flow Through Screens", Trans. ASME Vol.73 July
- Blair, M.F., Bailey, D.A., Schlinker, R.H. (1981), "Development of a Large-Scale Wind Tunnel for the Simulation of Turbomachinery Airfoil Boundary Layers", ASME Paper 81-GT-6
- Blair, M.F., Werle, M.J. (1980), "The Influence of Free-Stream Turbulence on Zero Pressure Gradient Fully Turbulent Boundary Layer", UTRC Report R80-9143388-12
- Cornell, W.G. (1958), "Losses in Flow Normal to Plane Screens", Trans. ASME Vol.80
- Dörr, Th. (1994), "Ein Beitrag zur Reduzierung des Stickoxidausstoßes von Gasturbinenbrennkammern", Dissertation TH Darmstadt
- Freudenberg, T. (1988), "Untersuchungen des Einflusses der Hauptstromturbulenz auf die ebene parallele Strahlmischung mit Hilfe eines neuartigen Turbulenzerzeugers", Dissertation, TH Darmstadt
- Gad-El-Hak, M., Corrsin, S. (1974), "Measurements on the nearly isotropic turbulence behind a uniform jet grid.", J.Fluid Mech. vol.62 part1 pp 115-143
- Gregory-Smith, D.G., Cleak, J.G.E. (1990), "Secondary Flow Measurements in a Turbine Cascade with High Inlet Turbulence", ASME Paper 90-GT-20
- Kiock, R., Laskowski, G., Hoheisel, H. (1982), "Die Erzeugung höherer Turbulenzgrade in der Meßstrecke des Hochgeschwindigkeits-Gitterwindkanals Braunschweig, zur Simulation turbomaschinenähnlicher Bedingungen", DFVLR-FB-82-85
- Kistler, A.L., Vrebalovich, T. (1966), "Grid Turbulence at Large Reynolds Numbers", J.Fluid Mech. Vol.26 part 1
- Kotlarski, T. (1980), "Erzeugung von höherer Turbulenzgraden bei Schaufelgitter-untersuchungen im Windkanal. Teil I: Turbulenz-graderhöhung in inkompressibler Strömung ohne Schaufelgitter", DFVLR IB 151-80/6
- Pinker, A.R., Herbert, M.U. (1967), "Pressure Loss Associated with Compressible Flow through Square-Mesh Wire Gauzes", J. of Mech. Ing. Vol.9 No.1
- Pinker, A.R., Herbert, M.U. (1966), "The pressure loss associated with compressible flow through square-mesh wire gauze", UDC 533.697:62-47 Report No.R281
- Rannacher, J. (1982), "Vorgang des Grenzschichtumschlags in laminaren Ablösewirbeln und seine Berücksichtigung bei Grenzschichtrechnungen", Maschinenbau-technik 31 pp.322
- Roach, P.E. (1987), "The generation of nearly isotropic turbulence by means of grids", Int. J. of Heat and Fluid Flow Vol.8 (2)
- Rosemann, H. (1989), "Einfluß der Geometrie von Mehrfach-Hitzdrahtsonden auf die Meßergebnisse in turbulenten Strömungen", Institut für Experimentelle Strömungsmechanik, DLR Göttingen DLR-FB-89-26
- Sturm, W., Fottner, L. (1985), "The High-Speed Cascade Wind Tunnel of the German Armed Forces University Munich", 8th Symp. on Meas. Tech. for Transonic and Supersonic Flows in Cascades and Turbomachines, Genoa
- Tasso, Y., Kamotani, Y. (1975), "Experiments on turbulence behind a grid with jet injection in downstream and upstream direction", The Physics of Fluids Vol.18 No.4
- Wunderwald, D., Wilfert, G., Fottner, L. (1992), "The Experimental Set-Up of a Triple-Sensor Anemometry and its Controlling System at the High-Speed Cascade Wind Tunnel", 11<sup>th</sup> Symposium on Measurement Techniques for Transonic and Supersonic Flow Cascades in Turbomachinery, München